

Magnetic Field Induced Exotic Phases in Isotropic Frustrated Spin-1/2 chain

Aslam Parvej* and Manoranjan Kumar†

S. N. Bose National Centre for Basic Sciences, Calcutta, Calcutta 700098, India

(Dated: May 14, 2019)

The frustrated isotropic $J_1 - J_2$ model with ferromagnetic J_1 and anti-ferromagnetic J_2 interactions in presence of an axial magnetic field shows many exotic phases, such as vector chiral and multipolar phases. The existing studies of the phase boundaries of these systems are based on the indirect evidences such as correlation functions *etc.* In this paper, the phase boundaries of these exotic phases are calculated based on order parameters and jumps in the magnetization. In the strong magnetic field, Z_2 symmetry is broken, therefore, order parameter of the vector chiral phase is calculated using the broken symmetry states. Our results obtained using the modified density matrix renormalization group and exact diagonalization methods, suggest that the vector chiral phase exist only in narrow range of parameter space J_2/J_1 .

PACS numbers: 75.10.Jm, 64.70.Tg, 73.22.Gk

I. INTRODUCTION

Frustrated quantum spin systems has been a frontier area of studies due to the existence of various exotic ground states. The realizations of low dimensional spin- $\frac{1}{2}$ systems such as quasi-one dimensional edge-sharing chain cuprates such $(N_2H_5)CuCl_3$ [1], $LiCuSbO_4$ [2] and $LiCuVO_4$ [3], where quantum effect are significant have intensified this area of research. Most of these magnetic systems are modelled by the isotropic $J_1 - J_2$ spin- $\frac{1}{2}$ model with J_1 antiferromagnetic [4–12] or ferromagnetic interaction [13–18]. This model in an axial magnetic field h can be written as

$$H(g) = \sum_p (J_1 \mathbf{S}_p \cdot \mathbf{S}_{p+1} + J_2 \mathbf{S}_p \cdot \mathbf{S}_{p+2}) - h \sum_p S_p^z \quad (1)$$

where J_1 and J_2 are nearest and next nearest neighbour interaction strength and h is strength of the axial magnetic field. The competition between these two parameters can lead to frustration in the systems if J_2 is anti-ferromagnetic [4–13, 15–19]. The systems with ferromagnetic J_1 interaction are relatively new and less studied theoretically, and especially the of effect of axial magnetic field [20–24] in ferromagnetic J_1 is poorly understood.

Recently synthesized one dimensional (1D) chain compounds, such as $LiCuSbO_4$, $LiCuVO_4$, Li_2ZrCuO_4 [25] and quasi-1D like $Ba_3Cu_3In_4O_{12}$ and $Ba_3Cu_3Sc_4O_{12}$ [26, 27] have ferromagnetic J_1 interactions. Some of these compounds, like $LiCuSbO_4$ does not have three dimensional ordering till 3 K and are very suitable for studies of low temperature behaviour of the compound. Other compounds like Li_2ZrCuO_4 , $LiCuSbO_4$ and

$LiCuVO_4$ are 1D systems with very small three dimensional ordering temperature T_{3D} , and have interaction strength ratio $J_2/J_1 \sim -0.45, -3.0$ and about -0.25 respectively. Some of these compounds like $LiCu_2O_2$ show multiferroic behaviour below a critical temperature [28].

In last decade, a remarkable amount of theoretical studies of $J_1 - J_2$ models with ferromagnetic J_1 have been done [20–24], still there is no consensus on the quantum phase diagram in large $|J_2/J_1|$ limit in the absence of magnetic field [12]. At $T = 0$, the ground state of the $J_1 - J_2$ model has ferromagnetic Tomonaga-Luttinger liquid phase with a quasi-long range order in the systems for $J_2/J_1 < -0.25$ and bond order wave phase (BOW) coexisting with spiral phase for $J_2/J_1 > -0.25$ [16–19]. The quantum phase diagram of the model at the finite axial magnetic field is playground of the exotic quantum phases [20–24]. Using bosonization procedure, Chubukov suggested that the ground state (gs) has an uniaxial dimerized and a biaxial spin Nematic phase [20]. In the above phases, rotation symmetry through the sites or through the bond are broken respectively [20]. Hikihara *et al.* used bosonization technique, exact diagonalization (ED) and density matrix renormalization group (DMRG) method to calculate the different phases in presence of the magnetic field. They predicted vector chiral (VC) and multi-polar phases in presence of strong magnetic field [21, 22]. Sudan *et al.* also showed the presence of the VC and the multipolar phases using the ED. They have used the square of VC order parameter and structure factor to construct the quantum phase diagram [23]. Most of these quantum phase diagrams are constructed on the basis of correlation functions especially the VC phase, [22–24] where square of the order parameter and different kind of correlation functions are calculated.

In this paper, we will concentrate on the VC and the multipolar phases of Hamiltonian H of Eq. 1. This paper

* aslam12@bose.res.in

† manoranjan.kumar@bose.res.in

is organized as follows; in section **II**, we discuss about the VC, multipolar phases and different broken symmetries in these phases. Results are presented in section **III** and discussed in section **IV**.

II. VECTOR CHIRAL AND MULTIPOLAR PHASES

VC phase is an interesting phase with spontaneous spin parity and inversion symmetry broken [16]. Order parameter of this phase can be written as

$$\langle \kappa \rangle = \langle \mathbf{S}_i \times \mathbf{S}_j \rangle \quad (2)$$

Where i, j are the neighbouring sites. This equation can be derived from the equation of motion [22] and the z-component of the above can be defined as follows,

$$\kappa_r^z = \langle \mathbf{S}_i \times \mathbf{S}_{i+r} \rangle^z = \frac{i}{2} [S_i^+ S_{i+r}^- - S_i^- S_{i+r}^+] \quad (3)$$

where, S_i^+ and S_{i+r}^- are the spin raising and lowering operators at site i . The z-component is just an anti-symmetric combination of bond order operators. For non-zero expectation values of the spin current, the Z_2 symmetry should be broken, *i.e.*, the system chooses a particular direction of the spin current spontaneously [22]. The Z_2 symmetry can also be broken by applying the Dzyaloshinskii-Moriya (DM) interaction.

The spin parity of Hamiltonian in Eq. 1 is not conserved in case of high field, where non-zero S^z spin is the gs, therefore, only inversion symmetry is broken to have the VC phase. In these systems, spontaneous inversion symmetry is broken if the gs is doubly degenerate. The expectation value of the order parameter, in this case, is spin current as defined in the Eq. 3 can be calculated as

$$\kappa_r^z = \langle \psi_+ | (\mathbf{S}_i \times \mathbf{S}_{i+r})^z | \psi_- \rangle \quad (4)$$

where $|\psi_+\rangle$ and $|\psi_-\rangle$ are the two degenerate ground states with opposite inversion symmetry. The chiral order parameter boundary with multipolar phase will be determined on the basis of non-zero values of κ^z .

The multipolar phase is another interesting phase in these systems. In presence of the high magnetic field, this model has variety of the multipolar phases. At $J_2/J_1 = -0.25$, the ferromagnetic and the singlet ground state are degenerate [16], *i.e.*, flipping of $\frac{N}{2}$ spin cost no energy, therefore, at this point of parameter space $p = \frac{N}{2}$ a multi-magnon state is stable. In the neighbourhood of the quantum critical point $J_2/J_1 = -0.25$, smaller p multi-magnon like $p = 6, 5, 4, 3, 2$ are stable states [22, 23]. All the higher p state phases are very narrow compare to $p = 3$ and 2 as shown by Hikihara *et al.* [22] and Sudan *et al.* [23]. We concentrate mostly on the Triatic ($p = 3$) and the Nematic ($p = 2$) phase. It

is shown that the Nematic phase is Tomonaga-Luttinger liquid (TL) of hard core bosons with two magnon bound states. Nematic phases are commensurate and incommensurate with momentum $q = \pi$ and q in the neighbourhood of π . In these phases both boson propagator and density-density correlation have the power law decay [22]. One can define a n-type spin Nematic order parameter[29] of this phase as

$$Q_{ij}^{\alpha\beta} = S_i^\alpha S_j^\beta + S_i^\beta S_j^\alpha - \frac{2}{3} \langle \mathbf{S}_i \cdot \mathbf{S}_j \rangle \delta_{\alpha\beta} \quad (5)$$

Where α and β are x,y and z component of the spin. As pointed out by Andreev and Grishchuk [30] and Hikihara [22] that

$$Q_{ij}^{x^2-y^2} = S_i^x S_j^x - S_i^y S_j^y, Q_{ij}^{xy} = S_i^x S_j^y + S_i^y S_j^x \quad (6)$$

$Q_{ij}^{x^2-y^2}$ and Q_{ij}^{xy} thought to be a quadrupolar spin operator. As pointed out by Chubukov that the Nematic order can be realized because of pairing of two-magnon excitations [20]. The Nematic order parameter can be redefined as $Q_{ij}^{\bar{-}} = Q_{ij}^{x^2-y^2} - iQ_{ij}^{xy} = S_i^- S_j^-$ where S_i^- is lowering spin operator at site i . Similarly, the order parameter of the higher order of multipolar phase can be redefined such as the octupolar Triatic $S_i^- S_j^- S_k^-$ and hexadecapolar $S_i^- S_j^- S_k^- S_l^-$ etc. These phase have been shown to exist in the magnetization plot by Hikihara *et al.* [22] and Sudan *et al.* [23]. Using the $Q_{ij}^{\bar{-}}$ as order parameter, the quadrupolar phase can be characterized by the jump of $\Delta S^z = 2$ in the magnetization vs. magnetic field.

III. RESULTS

In this paper, we study the quantum phase diagram of the $J_1 - J_2$ model and in an axial magnetic field. Exact diagonalization (ED) and modified density matrix renormalization group methods (DMRG) [8] are used to calculate the various results. The modified DMRG have better convergence than the conventional DMRG [31, 32]. The truncation error of density matrix eigenvalues of the DMRG calculation is less than 10^{-14} . DMRG is used for calculating various properties of large system up to 200 sites. The exact diagonalization method with inversion symmetries are used to determinations of energy levels crossing points for system sizes up to 28 sites. We are interested at absolute zero temperature, therefore, most of the calculations are done for the lowest states in each S^z manifolds.

We directly calculate the VC order parameter as defined in Eq. 4. The order parameter is sum of two operators with opposite sign and these operators are Hermitian conjugate of the each other therefore, the expectation value of both operators are same in a

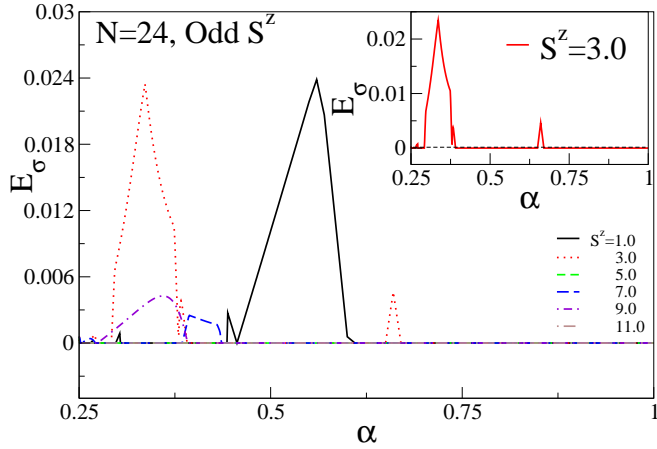


FIG. 1. Lowest excited states gap E_σ for odd S^z with the system size $N = 24$ is shown. Inset: Lowest excited states gap in a particular $S^z = 3.0$ sector for the system size $N = 24$.

non-degenerate state. States with non-zero VC order parameter κ has broken spin parity and the inversion symmetry. At sufficiently high magnetic field where the non-zero S^z is the gs, *i.e.* parity symmetry is already broken, therefore, just inversion symmetry should be broken in these states, and which can be done by taking as a linear combination of the degenerate gs with opposite inversion symmetry.

The expectation values of the order parameter are calculated as the matrix element between degenerate gs using Eq. 4, therefore, the degeneracy in gs in different S^z should be examined. To avoid the accuracy problem in case of small excitation gaps and to separate the two different symmetry subspaces, ED method with inversion symmetry is used. We have calculated the lowest gaps $E_\sigma = E(\sigma = 1) - E(\sigma = -1)$ where $E(\sigma = 1)$ and $E(\sigma = -1)$ are the lowest eigenvalues in a S^z sector with inversion subspace $\sigma = +$ and $\sigma = -$ respectively for different system sizes.

Fig. 1 shows the lowest excited states gaps E_σ for odd S^z sectors as a function of $\alpha = |J_2/J_1|$ with the system size $N = 24$. The inset of the Fig. 1 shows the E_σ for $S^z = 3$. We notice that there are multiple energy level crossings between $\alpha = 0.26$ and 0.67 . These crossings are at $0.261, 0.293, 0.391, 0.65$ and 0.67 . There are continuous degeneracy of the energy levels from $\alpha = 0.391$ to 0.65 and $\alpha > 0.67$. Whenever, doubly degenerate states become gs, continuous degeneracies are seen. The degenerate gs can be identified as $E_\sigma = 0$, and it is extended over range of α . In main figure, the E_σ for all the odd S^z sectors are shown. We notice that for smaller $\alpha < 0.7$, low magnetic S^z states are degenerate at multiple values of α . The multiple degeneracies for different values of the S^z corresponds to the multiple energy levels crossing, and are signature

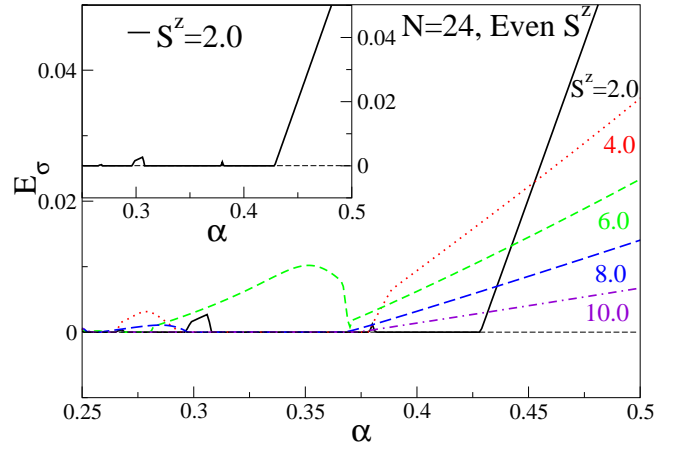


FIG. 2. Lowest excited states gap E_σ for even S^z of system size $N = 24$ is shown. Inset: Lowest excited states gap in a particular $S^z = 2.0$ sector for the system size $N = 24$.

of the spiral arrangement of the spins. Earlier it has been shown that spiral phase starts from $J_2/J_1 = -0.25$ at magnetic field $h = 0$ [19]. In finite system size, the energy levels become degenerate when the wavelength and size of the systems are commensurate. For large $|J_2/J_1|$, where chain can be treated as a zigzag chain, degeneracy in $S^z = 1$ state can be explained in terms of the decoupled phase like behaviour, where these two states have magnons localized at one of the two chains [11].

Similarly, Fig. 2 shows the lowest excited states gaps E_σ for even S^z sectors as a function of α with the system size $N = 24$ whereas, the inset of the Fig. 2 shows the lowest gap E_σ for $S^z = 2$. E_σ in this S^z sector shows similar pattern to that of the odd sectors in small α limit. There are degeneracy at $\alpha = 0.267, 0.272, 0.296, 0.308, 0.378, 0.381$ and 0.428 . There are continuous degeneracies from 0.308 to 0.378 and 0.381 to 0.428 . The large α limit, E_σ is finite *i.e.*, the lowest state is not degenerate which is contrary to the odd sector. In the main figure, all the even S^z sectors are shown. We notice that for all S^z sector, E_σ is finite at $\alpha > \alpha_c$. The α_c decrease with increasing the values of S^z .

TABLE I. Last energy levels crossing points α_c for different system sizes N in the even S^z sector are shown. α_c for few low S^z are extrapolated using the quadratic equations.

S^z	$N(16)$	$N(20)$	$N(24)$	$N(28)$	$N(\infty)$
2	0.394	0.412	0.428	0.440	0.54
4	0.375	0.376	0.378	0.380	0.39
6	0.370	0.368	0.370	0.373	0.38
8	-	0.372	0.367	0.367	-
10	-	-	0.373	0.370	-
12	-	-	-	0.374	-

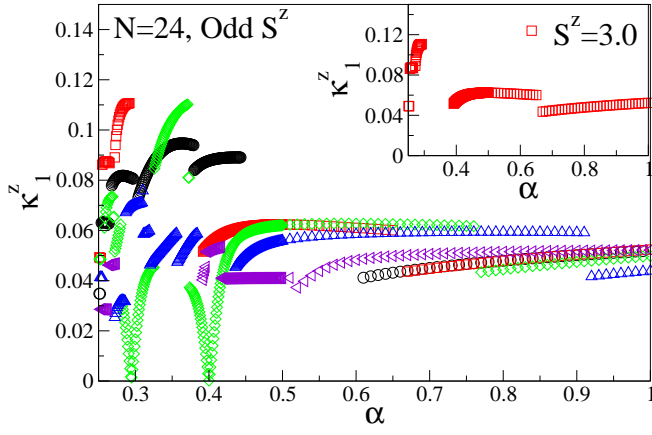


FIG. 3. Expectation values of the chiral vector order κ_1^z in the odd S^z sectors as a function of α with system size $N = 24$ is shown. Values of κ_1^z are calculated only at degenerate points. Inset: The expectation values of κ_1^z at a particular $S^z = 3.0$ sector as a function of α is shown. Black circle, red square, green diamond, blue triangle up, violet triangle left represent $S^z = 1, 3, 5, 7, 9$ respectively.

In table I, the last degeneracy points α_c of different even S^z sectors are listed. The ED calculations up to $N = 28$ site shows that the dependence of α_c on the system sizes is weak. The extrapolated values of α_c indicate that degeneracy of $S^z = 2, 4$ and 6 are extended to $\alpha_c = 0.54, 0.39$ and 0.38 respectively. The α_c for system size $N = 28$ in $S^z = 8, 10$ and 12 manifold are $0.367, 0.370$ and 0.374 respectively. Below α_c , the gs is degenerate, therefore, the broken symmetry states can be constructed by linear combination of these degenerate states.

The expectation values of the z -component of the chiral vector order parameter, κ_1 , is calculated using the Eq. 4, at degenerate points. For the system size $N = 24$, κ_1^z for odd S^z sectors are shown in the Fig. 3. In the inset of this figure, κ_1^z as function of α for $S^z = 3$ is shown. The values of κ_1^z is not a continuous function because of the energy levels crossings. When gs goes from one symmetry to other, κ_1^z values also change. As shown in inset, κ_1^z is continuous from 0.392 to 0.66 , and $\alpha > 0.67$. The energy levels in these interval are doubly degenerate as shown in inset of Fig. 1, and the discontinuity in the κ_1^z at 0.66 , is because of energy levels crossing. We notice that the variation of κ_1^z with the system size is weak. In the main Fig. 3, values of κ_1^z , between $\alpha = 0.25$ and 0.4 , have relatively higher values for smaller values of S^z . In the large α limit, κ_1^z in the all odd S^z sectors weakly depends on α .

The κ_1^z for all the even S^z is shown in Fig. 4. The κ_1^z for the $S^z = 2$ is shown in inset of the Fig. 4. The κ_1^z is discontinuous at four values of α and all the discontinuities occur at the energy levels crossings

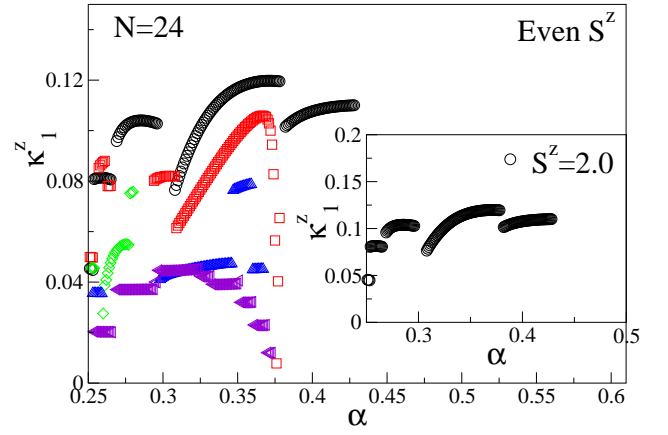


FIG. 4. Expectation values of the chiral vector order κ_1^z in the even S^z sectors as a function of α with the system size $N = 24$ is shown. Values of κ_1^z are calculated only at degenerate points. Inset: The expectation values of κ_1^z at a particular $S^z = 2.0$ sector as a function of α is shown. Black circle, red square, green diamond, blue triangle up, violet triangle left represents $S^z = 2, 4, 6, 8, 10$ respectively.

points. We notice that discontinuity point coincides with the energy levels crossing in inset of Fig. 2. κ_1^z of $S^z = 2$ is confined between $\alpha = 0.25$ and $\alpha \approx 0.45$, whereas this extend to higher values of α for $S^z = 3$. The main Fig. 4 shows that for all the even sector of S^z non-zero values of κ_1^z is confined below $\alpha = 0.5$ for this system size $N = 24$. Similar to odd S^z sector, values of κ_1^z in the small α limit, are large for smaller S^z . As we have stated earlier, κ_1^z is the order parameter for the VC phase, therefore, depending on the values of S^z of the gs in the strong magnetic field h , VC can be confined to less than 0.45 or extended to large values of the α for even or odd S^z respectively.

To understand the multipolar phases and finding the value of S^z in the gs at absolute zero temperature, we calculate the magnetization vs. magnetic field h ($M - h$ plot). Fig. 5 and 6 shows the magnetization vs. h plots for $\alpha = 0.35$ and $\alpha = 0.6$ respectively. In Fig. 5, $M - h$ curves for the system sizes $N = 24$ and $N = 48$ with periodic boundary condition (PBC) and $N = 48$ with open boundary condition (OBC) are shown in the main plots, whereas the inset shows the $M - h$ curves for OBC case with system sizes $N = 48$ and $N = 100$. For $\alpha = 0.35$, in PBC case, first few jumps in the magnetization are $\Delta S^z = 1$ and afterward the jumps are $\Delta S^z = 3$, and mediated by a small region of $\Delta S^z = 2$. The OBC system also have the similar trend that of PBC, except the magnetic field required to achieve same S^z in OBC case, is smaller compare to PBC case. As shown in inset of Fig. 5, jump of magnetization M is one up to $S^z = 7$ and $S^z = 18$ for system sizes $N = 48$ and $N = 100$ respectively. The lower arrow indicates the maximum value M up to which jump of 1 exist, whereas

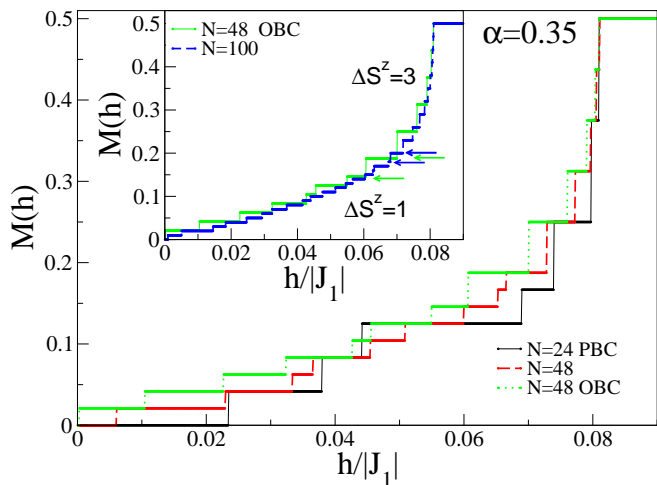


FIG. 5. Magnetization vs. axial magnetic field h for $\alpha = 0.35$ is shown. The calculations are done for system sizes $N = 24$ and $N = 48$ for the PBC and $N = 48$ for OBC. Inset: The $M(h)$ vs. h for the $N = 48$ and $N = 100$ for OBC is shown.

upper arrow indicates the beginning of jump of three. The jump of step of 2 exist between the two arrows. The boundary for jump of one and three can be at $M \approx 0.35$.

The magnetization M with different h , at $\alpha = 0.6$, is shown in the Fig. 6. Main figure shows the $M-h$ curves for both PBC and OBC. In OBC systems, magnetization start with jump one, but for $S^z > 2$, jumps in M are two till the saturation, whereas, jumps in the PBC systems, these jumps are always two. Inset of Fig. 6 shows that first two jumps in magnetization are always one. Based on the ED calculations for $N = 24$ for $\alpha = 0.35$, we notice that the degenerate lowest states are confined below the S^z manifold, as an example for $N = 24$ system size, all the even and odd gs are degenerate up to $S^z = 4$, whereas for higher values of h , gs is non-degenerate and jump in M is three *i.e.* the VC phase is confined below $S^z = 5$ and in the higher jump phase degeneracy is vanishes. Therefore, multipolar phase and chiral phase does not coexist. At higher field, $\Delta S^z = 3$ jumps indicates the octupolar phase or the Triatic order. The different system sizes with OBC, the similar trend are seen. In the thermodynamic limit, lowest states in low S^z manifold should be degenerate below α_c .

As shown in the Fig. 6, for $\alpha = 0.6$, magnetization jumps for the PBC with different system sizes are always $\Delta S^z = 2$. In the OBC case, initially magnetization jump is step of one up to $S^z = 2$ and $\Delta S^z = 2$ afterwards. Initial jumps of $\Delta S^z = 1$, is contradiction to that of $\Delta S^z = 2$ of PBC systems. The boundary of jump of one is shown by putting dashed line in the inset of the Fig. 6.

To resolve the issue, we have extrapolated the gaps $\Delta_1 = E(S^z = 1) - E(S^z = 0)$

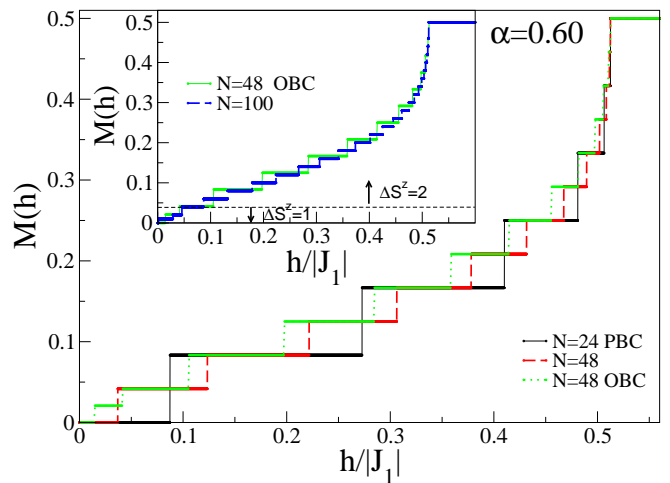


FIG. 6. Magnetization vs. axial magnetic field h for $\alpha = 0.60$ is shown. The calculations are done for system sizes $N = 24$ and $N = 48$ for the PBC and $N = 48$ for OBC. Inset: The $M(h)$ vs. h for the $N = 48$ and $N = 100$ for OBC is shown.

and $\Delta_2 = E(S^z = 2) - E(S^z = 0)$, where $E(S^z = 0)$, $E(S^z = 1)$ and $E(S^z = 2)$ are the lowest states in the $S^z = 0, 1$ and 2 spin sector respectively. In Fig. 7, Δ_1 and Δ_2 are shown as a function of $1/N$ for two different values of $\alpha = 0.6$ and $\alpha = 1.0$. Our extrapolated values of Δ_1 for both the values of α are less than 0.005. Extrapolated values of Δ_2 is 0.005 and 0.0006 for $\alpha = 0.6$ and 1.0 respectively. The above condition is true for all the values of $\alpha > 0.58$. Therefore, in the infinite systems, one can see only jumps of two in both PBC and OBC case. The extrapolated PBC and OBC results are consistent with each other.

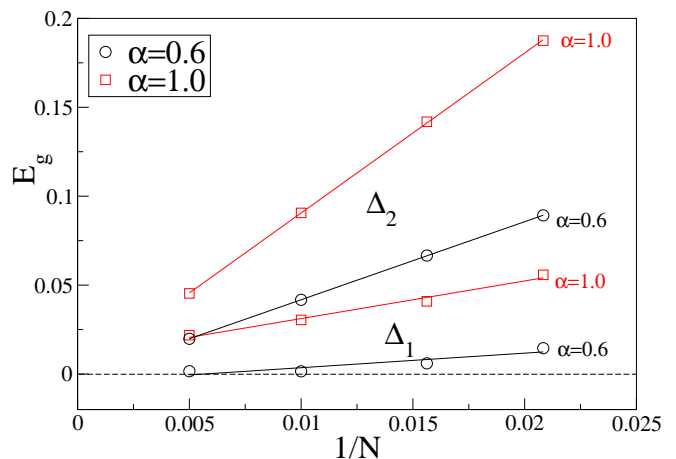


FIG. 7. For two values of $\alpha = 0.6$ and 1.0 , Δ_1 and Δ_2 are extrapolated where, $\Delta_1 = E(S^z = 1) - E(S^z = 0)$ and $\Delta_2 = E(S^z = 2) - E(S^z = 0)$, where $E(S^z = 0)$, $E(S^z = 1)$ and $E(S^z = 2)$ are the lowest states in the $S^z = 0, 1$ and 2 respectively.

Based on the above results, we agree with earlier calculations which show that $\alpha = 0.25$, the jump in magnetization is $\frac{N}{2}$ [16]. Systems goes from a fully polarized state $S^z = \frac{N}{2}$ to singlet gs. We also find that increasing α , value of multipolar order p decrease which is consistent to earlier results [22–24]. Our results for PBC systems with finite system size show that for $\alpha > 0.5$, jumps are always steps of 2 which is contrary to the earlier OBC results where $\Delta S^z = 2$ is followed by $\Delta S^z = 1$. As shown in the Fig. 6, for PBC systems with large α , only even S^z is stable gs, whereas all the odd states are skipped. Our DMRG calculations for system sizes up to 100 sites with PBC show that the gs for $\alpha > 0.56$ is always in sectors with even S^z . The extrapolated values of $\alpha_c = 0.54$ for the $S^z = 2$. The values of α_c decrease for higher S^z .

Based on the degeneracy and magnetization jumps, quantum phase diagram is shown in the Fig. 8. Our quantum phase diagram in $h - \alpha$ parameter space agrees with the existence of multipolar phases with $p = 2, 3$ and 4. We notice that the VC phase is confined to low magnetization whereas the multipolar phase is always a stable phase at higher magnetic field. For $N = 24$ sites calculations show that the degenerate gs have always magnetization jump of one, *i.e.*, $\Delta S^z = 1$. Therefore, the coexistence of the VC and the multipolar phase is avoided. Our phase boundary of quantum phase diagram, for $\alpha < 0.5$ are very similar to Hikiyama *et al.* but for higher values of α is different. As stated earlier, the VC phase is bounded by α_c values which are listed in table I. The boundary obtained from α_c and jump in the magnetization gives similar phase

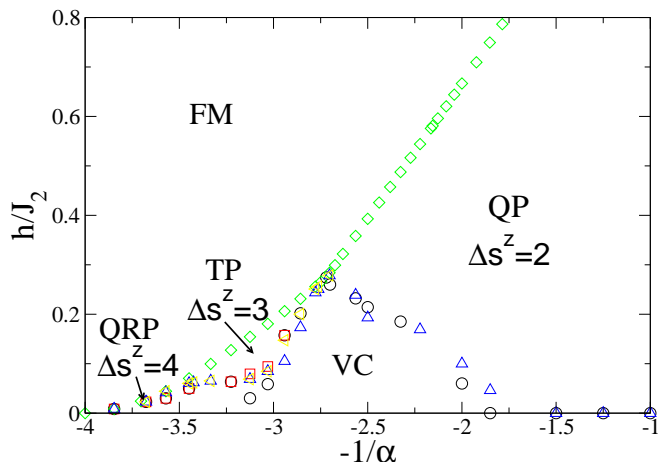


FIG. 8. Quantum phase diagram of $J_1 - J_2$ model in axial field is shown. Phase boundaries are obtained using OBC and PBC calculations. FM, QP, TP and QRP represents Ferromagnetic, quadrupolar, Triatic and Quartic phase respectively. Circle, Triangle boundary are calculated from PBC and OBC respectively.

boundary. The saturation magnetic field boundary is almost independent of the system size and is consistent with Hikiyama *et al.*

For large value of α in OBC, the finite size effect is very dominant. Finite system with PBC and OBC have different phase boundary but extrapolated values of the phase boundary of the VC phase and the quadrupolar phase is same. We notice that for $0.31 < \alpha < 0.37$, the VC phase and the Triatic phase boundary is mediated by the very small region of dipolar phase.

IV. DISCUSSION

Numerical approach is applied to study the isotropic $J_1 - J_2$ model with ferromagnetic J_1 in an axial magnetic field h . In these systems, Z_2 symmetry is spontaneously broken in the presence of an axial magnetic field [22–24]. As discussed earlier, the VC phase have been characterized based on various kind of correlation functions, like, current current correlation function, scalar chiral correlation *etc.*. The scalar chiral vector operator which involves three operators. The z -component of the $\mathbf{S}_i \cdot (\mathbf{S}_j \times \mathbf{S}_k)$ can be written as $S_i^z (S_j^+ S_k^- - S_j^- S_k^+)$ [33]. The evaluation of scalar chiral vector operator can be misleading in the case of finite systems with finite S^z values as it can give non-zero values even in non chiral phase.

For the first time, we show that the order parameter κ can be calculated using the broken symmetry states for this model, and also first time show that there are degeneracy in lowest states of $S^z \neq 0$ states. This method gives us direct evidence of the VC phase. The calculation of κ can be useful in calculating the electronic polarization $\mathbf{P} \propto \kappa$ in the improper Multiferroic materials such as $LiCuVO_4$ [3, 4]. We have constructed a new quantum phase diagram using the ED and the modified DMRG method. Our results below $\alpha < 0.5$ agree very well with the old results [22–24]. These results also suggest that $\alpha > 0.58$, only quadrupolar phase exists, whereas earlier results show the existence of the VC in low magnetic and the quadrupolar phase in the high magnetic field [22]. These conclusions are based on various criterion such as the magnetic jump in the field is always $\Delta S^z = 2$ for $\alpha > 0.58$. The last degeneracy crossing point's extrapolation value, shown in table I, is $\alpha \approx 0.54$. As shown in Fig. 7, systems with $\alpha = 0.6$ for OBC case, the field h required for going from $S^z = 0$ to 2 is below the numerical accuracy of the calculations. Therefore magnetic jump for $\alpha > 0.58$ is always 2, which indicates the existence of the quadrupolar phase.

At large α , systems goes to the decoupled phase limit, where the zigzag chain behaves like two regular Heisenberg chains. It is well known that in the thermodynamical limit of a regular Heisenberg chain, the

singlet and the triplet gap is zero [5–7]. In this limit, the lowest magnetic excitation on each chain is lowest singlet-triplet gap, but the total change in S^z is two for the two decoupled chains. Therefore excitation from gs to $S^z = 2$ sector of this system does not cost any energy. The extrapolated values of $\Delta S^z = 2 \approx 0$, in Fig. 7 also suggest the same. On the basis of above results,

we conclude that the VC phase exist only in the very narrow range of the parameter space.

Acknowledgements MK thanks DST for Ramanujan fellowship grant vide No. SERB/F/3290/2013-2014. MK thanks Z.G Soos for useful discussion and reading the manuscript carefully. MK also thanks S. Ramasesha and D Sen for the discussion.

-
- [1] N.Maeshima, M.Hagiwara, Y.Narumi, K.Kindo, T.C Kobayashi and K.Okunishi, *J. Phys.: Condens. Matter* **15**, 3607 (2003).
- [2] S. E. Dutton, M. Kumar, M. Mourigal, Z. G. Soos, J.-J. Wen, C. L. Broholm, N. H. Andersen, Q. Huang, M. Zbiri, R. Toft-Petersen, and R. J. Cava, *Phys. Rev. Lett.* **108**, 187206 (2012).
- [3] M. Mourigal, M. Enderle, B. Fak, R. K. Kremer, J. M. Law, A. Schneidewind, A. Hiess, and A. Prokofiev, *Phys. Rev. Lett.* **109**, 027203 (2012).
- [4] C. K. Majumdar and D. K. Ghosh, *J. Math. Phys.* **10**, 1388 (1969).
- [5] S.R.White and I.Affleck, *Phys.Rev. B* **54**, 9862 (1996); R. Chitra, Swapan Pati, H. R. Krishnamurthy, Diptiman Sen and S. Ramasesha, *Phys. Rev. B* **52**, 6581 (1995).
- [6] C. Itoi and S. Qin, *Phys. Rev. B* **63**, 224423 (2001).
- [7] M.Kumar, S. Ramasesha, D.Sen and Z. G. Soos, *Phys. Rev. B* **75**, 052404 (2007).
- [8] M.Kumar, Zoltan G. Soos, D.Sen and S. Ramasesha, *Phys. Rev. B* **81**, 104406 (2010).
- [9] M.Kumar, S. Ramasesha and Z. G. Soos, *Phys. Rev. B* **81**, 054413 (2010).
- [10] A. W. Sandvik, *AIP Conf. Proc.* 1297, **135** (2010) and references therein.
- [11] M.Kumar and Z.G. Soos, *Phys. Rev. B* **88**, 134412 (2013).
- [12] M.Kumar, A.Parvej and Z.G. Soos, arXiv:1405.1578, (2014).
- [13] F. Heidrich-Meisner, A. Honecker and T. Vekua, *Phys. Rev. B* **74**, 020403R (2006).
- [14] B Danu, B Kumar and R V. Pai, *EPL*, **100**, 27003 (2012).
- [15] I. P. McCulloch, R. Kube, M. Kurz, A. Kleine, U. Schollwöck and A. K. Kolezhuk, *Phys. Rev. B* **77**, 094404 (2008).
- [16] D. V. Dmitriev and V. Ya. Krivnov, *Phys. Rev. B* **73**, 024402 (2006).
- [17] J. Sirker, *Phys. Rev. B* **81**, 014419 (2010).
- [18] S. MahdaviFar, *J.Phys. Condens.Matter* **20**, 335230 (2008).
- [19] M. Kumar and Z. G. Soos, *Phys. Rev. B* **85**, 144415 (2012).
- [20] A. V. Chubukov, *Phys. Rev. B* **44**, 4693 (1991).
- [21] L.Kecke, T. Momoi and A. Furusaki, *Phys. Rev. B* **76**, 060407R (2007).
- [22] T. Hikihara, L.Kecke, T.Momoi and A.Furusaki, *Phys. Rev. B* **78**, 144404 (2008).
- [23] J. Sudan, A. Luscher and A. M. Läuchli, *Phys. Rev. B* **80**, 140402(R) (2009).
- [24] F. Heidrich-Meisner, I. P. McCulloch and A. K. Kolezhuk, *Phys. Rev. B* **80**, 144417 (2009).
- [25] S.L.Drechsler, O.Volkova, A. N.Vasiliev, N.Tristan, J.Richter, M.Schmitt, H.Rosner, J.Malek, R. Klingeler, A. A. Zvyagin and B.Büchner, *Phys. Rev. Lett.* **98**, 077202 (2007).
- [26] S.E Dutton, M.Kumar, Z.G Soos, C.L Broholm and R. J Cava, 2012 *J. Phys.: Condens. Matter* **24**, 166001 (2012); M.Kumar, S.E Dutton, R.J Cava and Z.G Soos, *J. Phys.: Condens. Matter* **25**, 136004(2013).
- [27] O. S. Volkova, I. S. Maslova, R. Klingeler, M. Abdel-Hafiez, Y. C. Arango, A. U. B. Wolter, V. Kataev, B. Büchner and A. N. Vasiliev, *Phys. Rev. B* **85**, 104420 (2012).
- [28] S.Park, Y.J.Choi, C.L.Zhang and S-W Cheong, *Phys. Rev. Lett* **98**, 057601 (2007).
- [29] N.Shannon, T.Momoi and P.Sindzingre, *Phys. Rev. Lett* **96**, 027213 (2006).
- [30] A. F. Andreev and I. A. Grishchuk, *Sov. Phys. JETP* **60**, 267 (1984).
- [31] S.R.White, *Phys. Rev. Lett.* **69**, 2863 (1992); *Phys. Rev. B* **48**, 10345 (1993).
- [32] K. Hallberg, *Advances in Physics*, **55**, 477 (2006); *U. Schollwöck Rev. Mod. Phys.* **77**, 259 (2005).
- [33] K. A. Al-Hassanieh, C. D. Batista, G. Ortiz and L. N. Bulaevskii, arXiv:0905.4871 (unpublished).